Comparison of Different Color Spaces for Image Segmentation using Graph-cut

Xi Wang[1], Ronny Hänsch[2], Lizhuang Ma[1] and Olaf Hellwich[2]
[1]*School of Electronic, Information and Electrical Engineering Shanghai Jiao Tong University, 800 Dong Chuan Road, 200240 Shanghai, P.R.China*
[2]*Computer Vision and Remote Sensing Group, Technical University of Berlin, Marchstr. 23, 10587 Berlin, Germany*
nicole.xiwang@gmail.com, r.haensch@tu-berlin.de, ma-lz@cs.sjtu.edu.cn, olaf.hellwich@tu-berlin.de

Keywords: Graph-cut, Color Space, Image Segmentation.

Abstract: Graph-cut optimization has been successfully applied in many image segmentation tasks. Within this framework color information has been extensively used as a perceptual property of objects to segment the foreground object from background. There are different representations of color in digital images, each with special characteristics. Previous work on segmentation lacks a systematic study of which color space is better suited for image segmentation. This work applies the Graph Cut algorithm for image segmentation based on five different, widespread color spaces and evaluates their performance on public benchmark datasets. Most of the tested color spaces lead to similar results. Segmentations based on L*a*b* color space are of slightly higher or similar quality as all the other methods. In contrast, RGB-based segmentations are mostly worse than a segmentation based on any other tested color space.

1 INTRODUCTION

Color, as a visual perceptual property of objects, is important in image coding, computer graphics, image as well as video processing, and many more computer vision tasks. Given the different needs of those application areas, different methods are used to represent color, each based on different mathematical ideas, with different advantages and limitations. Object segmentation has been deeply studied since 1970s (R. Ohlander and Reddy, 1978) and is a well-developed field within image processing. A segmentation system derives a partition of a given image into a set of (disjoint) regions. One particular case is foreground-segmentation (FGS), where one or multiple objects are considered as foreground and the rest of the image is labeled as background. FGS plays an important role in filmmaking as well as in photo and video editing. It is also used as an intermediate result for optical flow (T. Brox and Malik, 2009) and object recognition (C.H. Gu and Malik, 2009).

As one of the fundamental properties of objects, color has been used as important cue in several object segmentation frameworks (P. Arbelaez and Malik, 2011; J. Shotton and Criminisi, 2009). Given the range of needs of those methods as well as the various properties of existing color spaces, it is uncertain which color space fits an individual segmentation framework best and can lead to high performance.

During the last years graph-cut image segmentation has drawn a lot of attention and has for example been applied to medical image analyzation (Boykov and Jolly, 2001), color image segmentation (C. Rother and Blake, 2004), and remote sensing image segmentation (Sun and He, 2009). The Graph-Cut (GC) optimization framework (Boykov and Funka-Lea, 2006) belongs to the category of segmentation approaches, that are based on energy minimization. It allows the usage of global as well as local knowledge and constraints, where other segmentation approaches concentrate on only one of them.

The aim of this work is to provide some insight into the benefits and limitations of different color representations, when included as local and global cue into the GC segmentation framework as introduced in (Boykov and Funka-Lea, 2006). For this goal color is used as only cue, although other features like texture are undoubtedly able to provide important information for the segmentation process.

Segmentation is an ill-posed problem. The actual quality of any given segmentation can only be judged with respect to the final application. For example whether or not an object recognition system can benefit from the segmentation. Nevertheless, a good

segmentation should inhibit some important properties. Most importantly, the set of object boundaries in the image should be a subset of the segment boundaries, i.e. no segment covers both, fore- and background. In order to provide an objective measure of performance in this comparative study, the GC segmentation based on different color spaces is applied to images from the Berkeley Segmentation Benchmark (P. Arbelaez and Malik, 2011). In addition to a wide range of images, this database provides manually labelled reference data. The results do not only depend on the used color space, but also on the actual image content. Thus, a second set of experiments is conducted on the MSRC database (J. Shotton and Criminisi, 2009), where individual objects within the images are marked. The evaluation is carried out by comparing the obtained segmentation results to the reference data from those two benchmark datasets.

2 COLOR SPACE

There are many different color spaces proposed in the literature, each with its own properties, advantages, limitations, and areas of application. This work concentrates on five common examples, which are often used in image processing tasks: RGB, HSV, L*a*b*, L*u*v*, and the opponent color space. In order to evaluate whether color information is meaningful at all, a simple grayscale image representation is included as sixth "color" space.

Due to its simplicity the RGB color space is most commonly used. It is represented by red (R), green (G), and blue (B) chromaticities. The final color is defined by the additive combination of those three primary colors.

The Hue, Saturation, and Value (HSV) color space separates the intensity from the chromaticity and represents them independently. Hue describes the position of the color in a 360° spectrum. Saturation describes the pureness of the color: it measures the difference between the color and a grayscale value of equal intensity. Value, as the third channel, is the measurement of brightness.

The CIE L*a*b* and CIE L*u*v* spaces are selected to represent a uniform color space. These two color spaces are derived from the CIE XYZ color space and attempt to produce a coordinate system in which perceptual distances correspond to Euclidean distances (Judd and Wyszecki, 1975). In CIE L*a*b* color space, L* represents the lightness of color going from 0 (dark) to 100 (white), while the a* and b* channels are the two chromatic components. The first of these two (a*) represents the colors position between red/magenta (+a) and green (-a). Similarly, b* indicates its position between yellow (+b) and blue (-b). In practice, their range goes from -128 to 127 with 256 levels. Similar to L*a*b*, the CIE L*u*v* color space has one lightness channel and two chrominance components referring to the same chrominances. However, their transformation differs from L*a*b*. The range for u* component goes from -134 to 220 and -140 to 122 for v* component. The advantage of L*u*v* color space is, that it has a more linear transformation in the hue plane than L*a*b* color space, however, these two are roughly equivalent in representing a uniform perceptual color space.

The opponent color space has been claimed to give better performance in several image processing tasks (K. van de Sande and Snoek, 2008; Weijer and Gevers, 2005). In this space, two channels, O_1 and O_2 , are used to store the red-green and blue-yellow opponent pairs, while the O_3 channel is equal to the intensity channel in the HSV color space (K. van de Sande and Snoek, 2008). Its transformation is given by:

$$\begin{pmatrix} O_1 \\ O_2 \\ O_3 \end{pmatrix} = \begin{pmatrix} \frac{R-G}{\sqrt{2}} \\ \frac{R+G-2B}{\sqrt{6}} \\ \frac{R+G+B}{\sqrt{3}} \end{pmatrix} \quad (1)$$

3 GRAPH-CUT FRAMEWORK

The graph-cut framework proposed in (Boykov and Funka-Lea, 2006) is used as the fundamental object/background segmentation method in this work. In the graph model, each pixel is considered as a node and connected to its four neighbor nodes through edges. Edges between pixel nodes are called n-links. Additionally, there are two terminal nodes, S (source) and T (sink), which represent object and background, respectively. Each pixel node has two edges connected to S and T, which are called t-links. All links between two pixel nodes i and j are assigned with nonnegative weights w_{ij}. A cut through the graph is defined by the removal of edges and produces a bipartite graph in which there is no connected path from S to T. The cost $c(A,B)$ of this cut is calculated as:

$$c(A,B) = \sum_{i \in A, j \in B} w_{ij} \quad (2)$$

where A and B correspond to the two disjoint sets of nodes of the resulting bipartition. The min-cut/max-flow algorithm finds the optimal cut with minimum cost. This framework gives a pixel-precise segmentation. Figure 4(a)) shows a simple example for 3×3

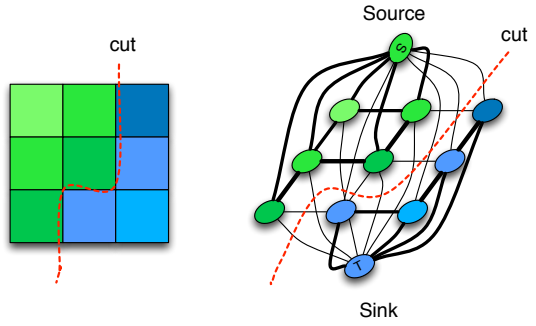

Figure 1: Segmentation example of a 3x3 image.

image, where the color information is used as cue to assign the edge weights.

GC segmentation is semi-supervised and relies on a small, manually labelled set of samples from fore- and background. A novel user interface is used in this work, which only requires a small fraction of the desired object region to be marked. Figure 4(a)) gives an example, where the red stroke marks the users selection to indicate the foreground object. The system then automatically estimates an approximate bounding box for the selected foreground object. Background seeds are sampled uniformly distributed from the outside-box area, while foreground seeds are selected within the bounding box. It is assumed that the region near the user-selected stroke has a higher probability to belong to the foreground object. Therefore, the foreground seeds are sampled according to a Gaussian distribution along the red stroke. In Figure 4 background seeds are marked in green and foreground seeds are marked in cyan.

The most crucial step of the whole framework is the assignment of edge weights. Based on the approach proposed in (Boykov and Funka-Lea, 2006), this work builds two Gaussian mixture models (GMM) from the sampled data of foreground (fg) and background (bg), respectively:

$$p(x|m) = \sum_{i=1}^{N_c^m} \alpha_i^m \cdot p(x|\mu_i^m \Sigma_i^m), \qquad (3)$$

where m corresponds to either foreground (fg) or background (bg), N_c^m is the number of components of the corresponding GMM, and $(\alpha_i^m, \mu_i^m, \Sigma_i^m)$ are the estimated parameters of the i-th component. They are used to predict the probability that a certain pixel is drawn from one of these two models. This probability is assigned as weight to the corresponding t-links of each node:

$$p(m|x) = \frac{p(x|m) \cdot P(m)}{p(x|fg) \cdot P(fg) + p(x|bg) \cdot P(bg)}, \qquad (4)$$

where $m \in \{fg, bg\}$. The prior probabilities are set to $P(fg) = P(bg) = 0.5$ in this work. The weights of the n-links w_{ij} are assigned based on the difference of color information between two pixels, i.e. the Euclidean distance $d(\cdot)$ of the color vector of two adjacents pixels x_i and x_j:

$$w_{ij} = \exp\left(-\frac{d(x_i, x_j)}{\sigma^2}\right). \qquad (5)$$

4 EXPERIMENTAL RESULTS

4.1 Motivation and Introduction

In general, segmentation is an ill-posed and mostly a rather subjective problem. The actual unbiased quality of a segmentation can only be judged in the context of the final application, e.g. object recognition. The second best way to evaluate a segmentation is to use some kind of manually defined reference data. However, image segmentation by humans is highly subjective, even if they agree on the kind (and number) of foreground objects. If there is already some variation in the definition of the reference data, it cannot be expected to obtain results by an (semi-)automatic method, which are in full agreement with this reference data. Furthermore, not the actual quality of the segmentation is tested, but the consistency with the manual segmentation. The assumption, that those two concepts are equivalent, might be invalid in many applications. Nevertheless, two publicly available benchmark datasets are used for evaluation in order to provide a fair comparison.

It should be emphasized that the goal of this work is not to achieve the best final segmentation, but to compare the potential of different color representations. There is a high color similarity between foreground and background in many images of the used datasets. A good segmentation of those cases cannot be achieved by color information alone. A realistic segmentation method would include other cues. One example are images of books or bikes. On the one hand, these objects show a large within-class color variation, which can be similar to the background. On the other hand, they have a clearly defined shape or structure.

In order to achieve an unbiased comparison of different color spaces, no other cue is used by the segmentation framework, i.e. no texture or shape features. Therefore, the results cannot be interpreted as absolute accuracy measurements. The above mentioned facts cause a high quality variation in the computed segmentations and the quality is expected to in-

crease when other features are taken into account. Instead, the results are relative measures providing information which color representation is more suited for image segmentation in general and specifically for graph-cut segmentation.

4.2 Settings

The main object of each image is selected as foreground, while the remainder is labelled as background. A manually marked stroke indicates the area from which foreground samples are taken as described above. In all experiments the same user input is used, i.e. the same stroke marks the foreground object.

In all the following experiments the same parameter settings are used. After transforming the given color image into the color space under investigation, the different image planes are normalized to the range of zero and one. This allows to fix the scale factor σ in Equation 5 to 0.2 for all color spaces. Both GMMs consist of five components and describe the joint probability in the respective three-dimensional color space. The parameters of each GMM are estimated by maximum likelihood from the samples of each class, respectively.

4.3 Performance Measures

It is seldom the case in FGS that the foreground is as large as the background. Mostly, one of those two classes dominates the image. That is why the main performance measurement used in this work to compare different segmentations with respect to the provided ground truth is the balanced accuracy (BA) (K.H. Brodersen and Buhmann, 2010) given by Equation 6. It avoids biased performance estimates caused by imbalanced data.

$$BA = (TPR + TNR)/2. \tag{6}$$

The true positive rate TPR (sensitivity) gives the percentage of correctly labelled foreground pixel and the true negative rate TNR (specificity) gives the percentage of correctly labelled background pixel.

The authors of (D. Martin and Malik, 2001) argued, that an error measure, which compares two given segmentations, should be robust regarding refinement, i.e. the error should be zero if one segment in the first segmentation is a subset of a segment in the second segmentation. If not, the error should be inversely proportional to the overlap of the two segments. In (D. Martin and Malik, 2001) the authors proposed the local refinement error as

$$E(S_1, S_2, p_i) = \frac{|R(S_1, p_i) \backslash R(S_2, p_i)|}{|R(S_1, p_i)|}, \tag{7}$$

where $R(S, p_i)$ is the pixel set of the segment in segmentation S, which contains pixel p_i, $\backslash$ denotes set difference and $|.|$ gives the cardinality of the set. This error is not symmetric. It is used to define two global error measures by forcing the refinement either globally in one direction (Global Consistency Error, GCE, Eq. 8), or allow for locally different directions of refinement (Local Consistency Error, LCE, Eq. 9):

$$GCE = \frac{1}{n} \min \left\{ \sum_{i=1}^{n} E(S_1, S_2, p_i), \sum_{i=1}^{n} E(S_2, S_1, p_i) \right\} \tag{8}$$

$$LCE = \frac{1}{n} \sum_{i=1}^{n} \left(\min\{E(S_1, S_2, p_i), E(S_2, S_1, p_i)\} \right) \tag{9}$$

4.4 Experiment on BSDS500

The first set of tests are conducted on the Berkeley segmentation dataset (BSDS500) benchmark (P. Arbelaez and Malik, 2011). This benchmark is originally not designed for FGS, but for general segmentation tasks. It consists of the 200 training and 100 test images from the former BSDS300, and adds 200 new test images, resulting in overall 500 images. GC segmentation is independently applied to individual images and no learning from other images takes place. That is why all 500 images are used.

For each of the images multiple segmentations are provided, which were manually generated by different humans. Those reference segmentations vary in quality, i.e. in accuracy of segment boundaries. To cast these general segmentations into the two class problem of FGS, the most dominant object or group of objects is selected as foreground, the remainder of the image as background, and all segments in the reference data are accordingly assigned to one of those two classes. Figure 2(a) shows one image example from this dataset along with one of the reference segmentations in Figure 2(b), as well as the two-class reference segmentation derived from it in Figure 2(c).

(a) (b) (c)

Figure 2: Image example from BSDS500. (a) original image and (b) reference segmentation shown in edges. (c) Two-class segmentation mask.

The above described segmentation framework is applied to each of the 500 images independently. For each image the mean value of the comparison of the

computed segmentation and the provided reference segmentations is computed. Table 1 shows the averaged mean values of each measurement for all 500 images in BSDS500. The best result is highlighted through boldface type. "Gray." stands for grayscale results and "Opp." stands for the opponent color space.

Table 1: Average BA, TPR, TNR, GCE, and LCE for all images in BSDS500.

	Gray.	RGB	HSV
BA	0.6951	0.7997	**0.8180**
TPR	0.6544	**0.7119**	0.7033
TNR	0.7357	0.8874	0.9327
GCE	0.2590	0.1893	**0.1601**
LCE	0.2103	0.1475	0.1181
	Opp.	L*u*v*	L*a*b*
BA	0.8152	0.8178	0.8163
TPR	0.6979	0.7000	0.6942
TNR	0.9324	0.9355	**0.9383**
GCE	0.1624	0.1612	0.1604
LCE	0.1202	0.1193	**0.1178**

The results clearly show the benefits of including color information over only using grayscale images. The usage of color, no matter in which representation, increased the accuracy by more than 10%.

The differences between the individual color spaces are considerably smaller. Among the tested representations, the RGB space is least suited for segmentation. Its accuracy is below 80% and thus more than 1.5% smaller than that of all the others. The TPR for RGB is 1% higher as for the other color spaces, but that comes at the cost of including too much of the background into the foreground segment, resulting in a much higher false-positive rate (or equivalently lower true-negative rate).

The remaining four color spaces lead very similar results with respect to all five measurements. The HSV color space gives the best overall accuracy and global consistency error of all 500 images, and the L*a*b* color space gives the lowest local consistency error. The differences are small but significant, which was tested by a two-tailed McNemar's test with a confidence level of 99%.

4.5 Experiment on MSRC

The BSDS500 dataset consists of unordered images of highly variant content. During the corresponding experiments it was noted that the segmentation results differed not only between different color spaces, but also depend on the particular image category. A color space that performed well for some image categories led to only inferior results for other types of images. In order to investigate this subject further a second benchmark dataset is used.

The MSRC dataset (J. Shotton and Criminisi, 2009) contains 591 images that are ordered into 20 different categories (e.g. animal, tree, building, etc.). Within each category the content of the individual images is similar. This dataset is designed for object recognition instead of segmentation. That is why it provides corresponding labelled reference images additionally to the image category label. The main object (according to the image category) was selected as foreground and the rest of the image as background. Figure 3(a) shows an example together with the provided reference image in Figure 3(b) and the generated foreground-segmentation mask in Figure 3(c).

(a) (b) (c)

Figure 3: Image example from MSRC. (a) original image and (b) label image. (c) Two-class segmentation mask.

Compared to the BSDS500 dataset, the images of the MSRC dataset have a rather simple content. The subjective segmentation is clearer, since the foreground object can be easier defined. Most images in MSRC have only one single object and the difference between background and foreground is clear. However, the reference images provide only a coarse object outline and are by far not as accurate as in BSDS500.

Table 2 presents the values of the performance measures obtained from the MSRC dataset averaged over all images regardless of their category.

The general findings of the previous subsection are confirmed by the results obtained by using the MSRC dataset. The usage of color leads to an large increase of accuracy compared to using only grayscale images. The worse performance of the RGB color space is even more obvious here. The remaining color spaces show again very similar behaviour.

Table 3 illustrates the BA averaged over all images for each of the twenty available categories. Since grayscale and RGB consistently performed worse, they are omitted. The classes are ordered by the BA value obtained by using L*a*b*, which is given in the last column. The columns corresponding to the

Table 2: Average BA, TPR, TNR, GCE, and LCE for all images in MSRC.

	Gray.	RGB	HSV
BA	0.7211	0.7961	0.8162
TPR	0.6436	0.6861	0.6990
TNR	0.7985	0.9061	0.9334
GCE	0.524	0.3481	0.2902
LCE	0.3911	0.2331	0.1732
	Opp.	L*u*v*	L*a*b*
BA	0.8176	0.8179	**0.8204**
TPR	0.6973	**0.6995**	0.6992
TNR	0.9379	0.9362	**0.9416**
GCE	0.2786	0.2814	**0.2732**
LCE	0.1606	0.1643	**0.1543**

other three color spaces show the difference value to the L*a*b* accuracy, where a negative value means that the method performed worse. The two last lines of the table count how often each color space outperformed all other color spaces (#best), and how often it resulted in better segmentations than L*a*b* (#better), respectively.

Table 3: Overall accuracy for 20 classes in MSRC.

Class	HSV	Opp.	L*u*v*	L*a*b*
Bike	-1.72	-0.81	-1.26	**71.84**
Chair	**0.05**	-0.56	-0.8	75.89
Street	-0.81	-1.62	**0.11**	77.44
Book	**1.2**	0	0.18	77.67
Car	0.19	**1.08**	0.56	78.58
Plane	-1.16	-0.22	**0.58**	80.58
Boat	-0.69	-0.33	**1.21**	80.63
Tree	**0.75**	0.53	-0.31	80.64
Sea	-2.02	-0.69	-0.78	**82.09**
Animal	0.16	0.35	**0.56**	83.26
Flower	**0.62**	0.07	-0.49	83.52
Dog	-0.22	-1.27	-0.19	**83.55**
Face	**0.56**	0.41	-0.08	83.83
Cow	-1.02	-0.12	**0.33**	83.94
Cat	-1.62	-1.97	-1.77	**84.19**
Bird	-0.94	-1.8	-1.77	**84.79**
Sheep	-0.1	**1.07**	-0.47	85.41
Building	-1.44	-0.25	-0.33	**86.14**
Person	-0.38	-0.06	-0.03	**86.3**
Sign	-0.41	**0.43**	-0.41	90.85
#best	25%	15%	25%	**35%**
#better	35%	30%	35%	-

The similarity of the individual accuracies of those four color spaces are again notable. Also the slight superior performance of L*a*b*, which outperformed each other color space in approximately 70% of all cases. It resulted in better segmentation than any other color space in still 35% of the cases. If L*a*b* is outperformed by another color space, then the difference in performance is on average smaller than if it led to better results. Thus, L*a*b* gives better results on average, although the difference is only small.

The relative ordering of the individual categories is also notable. All color spaces show the worst performance with "hard" classes like "Bike" and "Chair", which consists of many fine structures with considerable gaps in between. These gaps are included into the object area within the reference data, which leads to a mixture of fore- and background samples within the GC framework. The best performance is achieved for "easy" categories like the "Sign" class. These objects have clear boundaries, show only a limited set of colors which are designed to be distinct from the background, and have no noteable 3D structure which could lead to color changes due to inhomogeneous lighting. Apart from only a few exceptions this relative ordering is consistent with respect to the different color spaces.

Additional to the relative ordering of the classes based on the accuracy of the corresponding segmentation, they are also grouped into coarser semantic categories. One example is the "Vehicle" category, which consists of "Car", "Plane", and "Boat". Another even larger group consists of every animal class within the dataset (but includes "Flower" and "Face" as well). There are "radiometric" groups as well, which consists of object categories that show similar foreground-background statistics. One example is the aforementioned problem caused by the fine structures of chairs and bikes, which lead to a mixture of foreground and background samples. Another example are "Tree" and "Sea" categories. Images in those classes consists of a rather large foreground object, which has a very similar color to a huge part of the background (lawn in the tree class and the blue sky in the sea class).

Table 3 shows, that the segmentation accuracy indeed depends on the object category, but the differences are only small, i.e. less than 2% in all cases. There is no single best color space, although L*a*b* leads to slightly better results on average. The relative performance of different color spaces is not consistent for any of the groups discussed above. L*a*b* seems to be able to deal better with animal categories, where it is outperformed in three out of six cases, two times by the very similar L*u*v* color space. In general the results of these two color spaces are close to each other most of the time. The largest difference is caused by the bird and cat classes, where L*a*b* color space demonstrates a better ability to deal with illumination variance. Figure 4 illustrates segmenta-

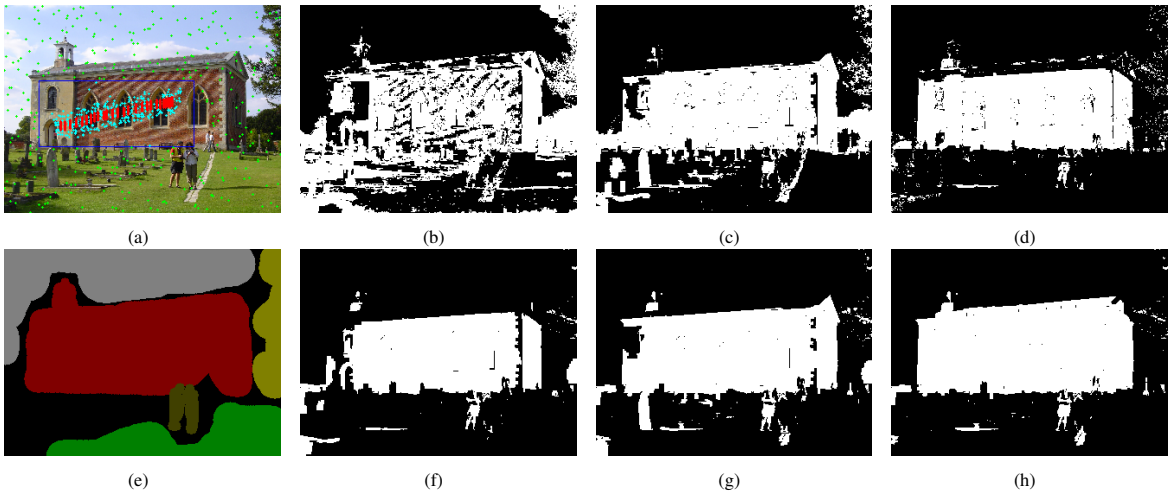

(a) (b) (c) (d)

(e) (f) (g) (h)

Figure 4: Segmentation results for a house image. (a) Original image with random selected sample seeds. (e) Reference image. (b) (c) (d) (f) (g) (h) are the segmentation results in Grayscale, RGB, HSV, opponent color space, L*u*v* and L*a*b* color spaces respectively. White area indicates the selected foreground.

tion results of a "Building" image. The L*a*b* color space gives the best result. It is robust to illumination changes and thus able to segment the shadow area of the house correctly. RGB, opponent color space and L*u*v* failed to correctly segment the left part of the building. The roof is segmented as part of the background in all the color spaces except L*a*b*.

4.6 Summary

The experiments clearly show that color is an important and very descriptive property of objects in images. Segmentation methods like GC greatly benefit from the usage of color instead of relying on grayscale images alone.

The results of all color spaces are close to each other. No color space actually failed to provide a meaningful segmentation. The results from both test sets suggest that L*a*b* is best suited for foreground segmentation. The intrinsic color component is better presented in L*a*b* color space. Therefore, it can deal better with shadow and other lighting changes. The difference to the second best color space is only small, but significant. The second best choice is either L*u*v* or HSV. RGB is the least suited color space in the tested FGS scenario.

The performance of the segmentation method does depend on the object category, in particular on relative statistics of fore- and background. Again, L*a*b* shows best results on average, but is outperformed by any of the other color spaces in 65% of the cases. However, the winning method is not consistently distributed over the other color spaces.

It should be noted, that the tested segmentation framework strongly depends on the Gaussian assumption. Gaussian mixture models are used to estimate the color model of fore- and background and the difference of two adjacent color pixel is measured by the Euclidean distance. L*a*b* and L*u*v* are designed so that the perceptual difference of individual colors is proportional to the distance in the corresponding three-dimensional vector space. This assumption is problematic for the HSV color space, where the hue values (as main component representing color) lie on a ring. It is also well known, that the perceptual difference of RGB colors does not correspond to the Euclidean distance within the RGB vector space. Nevertheless the Euclidean distance is commonly used and it is not a trivial task to design distance measures which better represent perceptual differences in those color spaces.

5 CONCLUSIONS AND FUTURE WORK

This paper provides a first comparative study of different color spaces in the context of image segmentation based on graph-cut. A GMM-based color model is automatically build to assign weights to the *t*-links, while an exponential transform of the Euclidean distance is used as *n*-links weight.

An easy-to-use user interface is provided to indicate the foreground object. Experiments are conducted in six color spaces: Grayscale, RGB, HSV, opponent color space, L*u*v*, and L*a*b*. The segmentation accuracy estimated over nearly 1100 different images shows on the one hand that there is

no overall best color space. The quality depends not only on the color space, but is as well data dependent, i.e. varies for different object classes. On the other hand L*a*b* shows a strong tendency to lead to good results, which compare favorably even in cases where other color spaces show a slightly higher performance.

The objective of this work is to study the impact of five different, commonly used color spaces on segmentation obtained by Graph-Cut. Future work will extend the current work mainly in four directions: Firstly, a larger range of color spaces will be included for comparison in order to provide a more exhaustive study on the topic and to improve the preliminary conclusions given in this work. Secondly, experiments will also be conducted using other semi-supervised image segmentation methods, such as fuzzy information fusion algorithm (Valet et al., 2001), decision forests (J. Shotton and Criminisi, 2009) and so on. Thirdly, a final segmentation approach should not be based on color alone. Instead other cues should be exploited as well. Texture will be included into the segmentation framework in order to study the interplay between those two complementary cues. For this purpose textons (Julesz, 1986) will be used to extract texture information, while the radiometric properties are captured by different color models. Fourthly, a more thoroughly analysis on the interdependence of different color spaces and image/object category on the segmentation results will be carried out.

ACKNOWLEDGEMENTS

This work is funded in part by National Natural Science Foundation of China No. 61133009 and No. 61073089.

REFERENCES

Boykov, Y. and Funka-Lea, G. (2006). Graph cuts and efficient nd image segmentation. *International Journal of Computer Vision*, 70(2):109–131.

Boykov, Y. Y. and Jolly, M. P. (2001). Interactive graph cuts for optimal boundary and region segmentation of objects in n-d images. *8th IEEE International Conference on Computer Vision*, 1:105–112.

C. Rother, V. K. and Blake, A. (2004). Grabcut: Interactive foreground extraction using iterated graph cuts. *ACM Transactions on Graphics (TOG)*, 23(3):309–314.

C.H. Gu, J. J. Lim, P. A. and Malik, J. (2009). Recognition using regions. In *IEEE Conference on Computer Vision and Pattern Recognition, CVPR*, pages 1030–1037.

D. Martin, C. Fowlkes, D. T. and Malik, J. (2001). A database of human segmented natural images and its application to evaluating segmentation algorithms and measuring ecological statistics. In *Eighth IEEE International Conference on Computer Vision*, volume 2, pages 416–423.

J. Shotton, J. Winn, C. R. and Criminisi, A. (2009). Textonboost for image understanding: Multi-class object recognition and segmentation by jointly modeling texture, layout, and context. *International Journal of Computer Vision*, 81(1):2–23.

Judd, D. B. and Wyszecki, G. (1975). *Color In Business*. John Wiley and Sons, London, 2nd edition.

Julesz, B. (1986). Texton gradients: The texton theory revisited. *Biological Cybernetics*, 54(4-5):245–251.

K. van de Sande, T. G. and Snoek, C. G. (2008). Color descriptors for object category recognition. In *In European Conference on Color in Graphics, Imaging and Vision*, volume 2, pages 378–381.

K.H. Brodersen, C.S. Ong, K. S. and Buhmann, J. (2010). The balanced accuracy and its posterior distribution. In *Proceedings of the 20th International Conference on Pattern Recognition*, pages 3121–3124.

P. Arbelaez, M. Maire, C. F. and Malik, J. (2011). Contour detection and hierarchical image segmentation. *IEEE Transactions on Pattern Analysis and Machine Intelligence*, 33(5):898–916.

R. Ohlander, K. P. and Reddy, D. R. (1978). Picture segmentation using a recursive region splitting method. *Computer Graphics and Image Processing*, 8(3):313–333.

Sun, F. and He, J. P. (2009). The remote-sensing image segmentation using textons in the normalized cuts framework. In *International Conference on Mechatronics and Automation (ICMA)*, pages 9–12.

T. Brox, C. B. and Malik, J. (2009). Large displacement optical flow. *IEEE Conference on Computer Vision and Pattern Recognition (CVPR)*, 41(48):20–25.

Valet, L., Mauris, G., Bolon, P., and Keskes, N. (2001). Seismic image segmentation by fuzzy fusion of attributes. *Instrumentation and Measurement, IEEE Transactions on*, 50(4):1014–1018.

Weijer, J. V. D. and Gevers, T. (2005). Boosting saliency in color image features. In *In Computer Vision and Pattern Recognition (CVPR)*, volume 1, pages 365–372.